A theoretical study of (old and new) non-classical carbocations derived from cyclic saturated hydrocarbons[†]

Ibon Alkorta,[1]* José Luis M. Abboud,[2]* Esther Quintanilla[2] and Juan Z. Dávalos[2]

[1]Instituto de Química Médica (CSIC), Juan de la Cierva 3, E-28006 Madrid, Spain
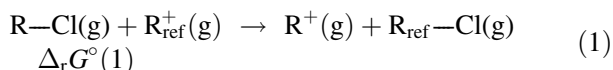[2]Instituto de Química Física 'Rocasolano' (CSIC), Serrano 119, E-28006 Madrid, Spain

epoc   ABSTRACT: Nine non-classical carbocations derived from cyclic saturated hydrocarbons were studied by means of *ab initio* calculation, MP2/6–311G**. The geometry, energetics, orbital interactions within the Natural Bond Orbital formalism, electron density and chemical shieldings were obtained and analyzed. In all cases a similar geometrical distribution ('non-classical moiety,' NCM) was obtained with the carbon atoms located in a triangle with two of their sides of 1.84 Å and the third of 1.40 Å. The energetic stability of the carbocations was rationalized on the basis of the strain in the rings involved. The NBO analysis shows that the charge is largely distributed over the three centers and also the existence of a two-electron, three-center orbital with similar contribution of the three atoms. Electron density maps were obtained and analyzed. In all cases, the chemical shieldings of the CH_2 group of the NCM are in the region of saturated hydrocarbons whereas those for the CH group are similar to those found in double-bonded systems. Copyright © 2003 John Wiley & Sons, Ltd.
*Additional material for this paper is available from the epoc website at http://www.wiley.com/epoc*

KEYWORDS: cyclic saturated hydrocarbons; non-classical cations; stability

INTRODUCTION

We have been involved for some time in the experimental determination of the intrinsic (gas-phase) stabilities of carbocations, R^+, by means of Fourier transform ion cyclotron resonance (FT-ICR) spectroscopy. A quantitative ranking of these stabilities is given by $\Delta_r G°$ (1), the standard Gibbs energy change for the chloride exchange reaction (1) in the gas phase:

$$R—Cl(g) + R_{ref}^+(g) \rightarrow R^+(g) + R_{ref}—Cl(g) \qquad (1)$$
$$\Delta_r G°(1)$$

where R_{ref}^+ is an arbitrarily chosen reference cation. This process has been consistently used in our previous work, 1-adamantyl (1-Ad$^+$) being selected as the reference ion, reaction (1a):

$$R—Cl(g) + 1\text{-}Ad^+(g) \rightarrow R^+(g) + 1\text{-}Ad—Cl(g) \qquad (1a)$$
$$\Delta_r G°(1a)$$
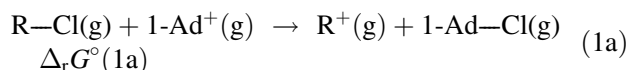
*Correspondence to: J. L. M. Abboud, Instituto de Química Física 'Rocasolano' (CSIC), Serrano 119, E-28006 Madrid, Spain.
E-mail: jlabboud@iqfr.csic.es
I. Alkorta, Instituto de Química Médica (CSIC), Juan de la Cierva 3, E-28006 Madrid, Spain.
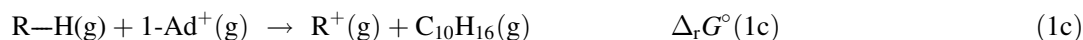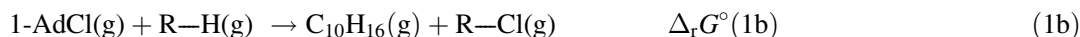E-mail: ibon@iqm.csic.es

The species hitherto examined include, among others, a number of bridgehead cations of widely different stabilities,[1] such as 1-norbornyl, 1-adamantyl (1-Ad$^+$) and manxyl (bicyclo[3.3.3]undecanylium cation), aliphatic,[2] aromatic[3,4] and bi- and tricyclic secondary cations.[4–6]

Some significant results derived therefrom are as follows.

First, let k and k_0 stand for the solvolysis rates of bridgehead chlorides R—Cl and 1-adamantyl chloride, 1-AdCl, respectively, in the same solvent and at the same temperature. We have shown that $\log(k/k_0)$ is linearly related to $\Delta_r G°$ (1a) to a very high degree of precision. The correlation spans some 25 log units in rates and 200 kJ mol^{-1} in Gibbs energies and includes, *inter alia*, bridgehead species and bi- and tricyclic secondary cations. These results are fully consistent with the concept that S_N1 solvolysis rates for a series of similar compounds under the same reaction conditions directly reflect the stability of their carbocationoid transition states.[7] They further indicate the relevance of the gas-phase thermodynamic data for the purpose of understanding solution reactivity. A referee has indicated that recent computational work suggests that the transition states for the solvolysis of 2-*exo*-norbornyl derivatives do not resemble the isolated cartion.[8] Also, we have long been aware of the fact that medium effects are able to reverse the ranking of carbocation stabilities determined in the gas phase.[9] This notwithstanding, the empirical

LFER indicated above exists, irrespective of mechanistic details, and has been of use in some cases.[2b]

Second, combination of the experimental value of $\Delta_r G°$(1a) with $\Delta_r G°$(1b), the standard Gibbs energy change for the isodesmic reaction (1b), provides $\Delta_r G°$(1c), the standard energy change for the hydride transfer process (1c):

$$1\text{-AdCl(g)} + \text{R—H(g)} \rightarrow \text{C}_{10}\text{H}_{16}\text{(g)} + \text{R—Cl(g)} \qquad \Delta_r G°\text{(1b)} \qquad (1b)$$

$$\text{R—H(g)} + 1\text{-Ad}^+\text{(g)} \rightarrow \text{R}^+\text{(g)} + \text{C}_{10}\text{H}_{16}\text{(g)} \qquad \Delta_r G°\text{(1c)} \qquad (1c)$$

where $\text{C}_{10}\text{H}_{16}$ is the adamantane hydrocarbon.

Reaction (1c) is relevant because (i) It also provides a quantitative ranking of carbocation stabilities, (ii) it can be studied experimentally in some cases and (iii) the absence of chlorine facilitates computations at relatively high levels.

Reactions (1a)–(1c) are isodesmic processes. Among them, reaction (1b) is seen to involve only neutral species. For most bridgehead and bicyclic chlorides the absolute value of $\Delta_r G°$ (1b) is small (below 10 kJ mol^{-1}) with respect to the overall range of structural effects. In our experience, calculations at the HF/6–31G(d) level provide satisfactory estimates of this 'leaving group correction' when the appropriate experimental information is not available. As regards the computational determination of $\Delta_r G°$(1c), we have used MP2/6–311G(d,p) and G2(MP2) levels. With these techniques, we have found that both purely computational and purely experimental $\Delta_r G°$(1c) values agree within an unsigned average difference of ca 8 kJ mol^{-1}. Furthermore, whenever $\Delta_r H°$(1c) values (readily determined from experimental $\Delta_r G°$(1c) values through the appropriate entropy corrections) could be compared to experimental data obtained by entirely different techniques, excellent agreement was obtained.[5,10]

Initially, most of our computational studies were simply aimed at cross-checking the experimental data. This led us to deal with some 'non-classical' ions. The Brown–Schleyer joint definition[11] of a non-classical carbocation is 'a positively charged species which cannot be represented adequately by a single Lewis structure. Such a cation contains one more carbon or hydrogen bridges joining the two electron-deficient centers. The bridging atoms have coordination numbers higher than usual, typically five or more for carbon and two or more for hydrogen. Such ions contain two electron-three (or multiple) center bonds including a carbon or hydrogen bridge.' Historically, camphenyl cation[12] provided the basis for the concept of non-classical ions to develop and still remains an important species in its own right.[13]

Although we have observed in previous work that a number of 'carbon bridges' display a nearly constant geometry, irrespective of the relative stabilities of the ions, we have never examined this topic in detail.[1,4–6] In this study, we considered the presence and properties of this common geometrical feature ('non-classical moiety,' NCM) in a set of various cations, formally non-classical and derived from secondary cations, of widely different geometric structures and sizes. Important theoretical studies have been published recently on these NCM particularly regarding their electronic properties, notably by Werstiuk and co-workers.[14]

We selected the following seven carbocations which, according to common usage, are 'non-classical' species: bicyclo[2.1.0]pent-2-ylium (**1b**$^+$), bicyclo[2.1.1]hex-2-ylium[15,16] (**2b**$^+$) norbornan-2-ylium[17] (**3b**$^+$), homoadamantan-4-ylium (**5b**$^+$), norbornan-7-ylium[18,19] (**7b**$^+$), bicyclo[2.2.2]oct-2-ylium[14a,17,20,21] (**8b**$^+$) and adamantan-2-ylium (**9b**$^+$). For comparison purposes, the methyl-substituted derivatives of **3b**$^+$ and **5b**$^+$, **4b**$^+$ and **6b**$^+$, respectively, were also examined.

As far as we are aware, information on **1b**$^+$ is not yet available. The intrinsic (gas-phase) stability and structure of **5b**$^+$ were studied experimentally and computationally very recently.[4,6] The 'non-classical' character of **9b**$^+$ was suggested in important computational work dealing with the protonation of adamantane.[22] It is interesting that, years ago, Sorensen and co-workers had already drawn attention to remarkable structural aspects of this ion[23] (for an important contribution to the field of non-classical carbocations, see Ref. 23b). **3b**$^+$ has played a key role in physical organic chemistry because of the vigorous academic discussion it generated[11,24] until a combination of low-temperature ^{1}H and ^{13}C NMR,[25] ^{13}C solid-state NMR,[26] solid-state FT-IR[27] and ESR[28] techniques established the bridged structure of this ion. A combination of high-level *ab initio* and Monte Carlo calculations indicate that this is also the only stable structure in solution.[29] The bridged structure of **8b**$^+$ has already been established.[14a]

Topics considered herein include the geometry, energetics, electron density and bonding within the NBO methodology and nuclear shieldings for the nine compounds mentioned above. The various ions examined in this work are summarized in Fig. 1.

METHODS

The computational level used in this work was obviously determined by the substantial size of many of the species examined. As rightly indicated by a referee, the MP2 level sometimes overestimates bridging in some systems.[30] In this work, however, we used the MP2/6–311G(d,p) level, the reasons being as follows. It has been pointed out that MP2/6–31G(d) or higher levels are
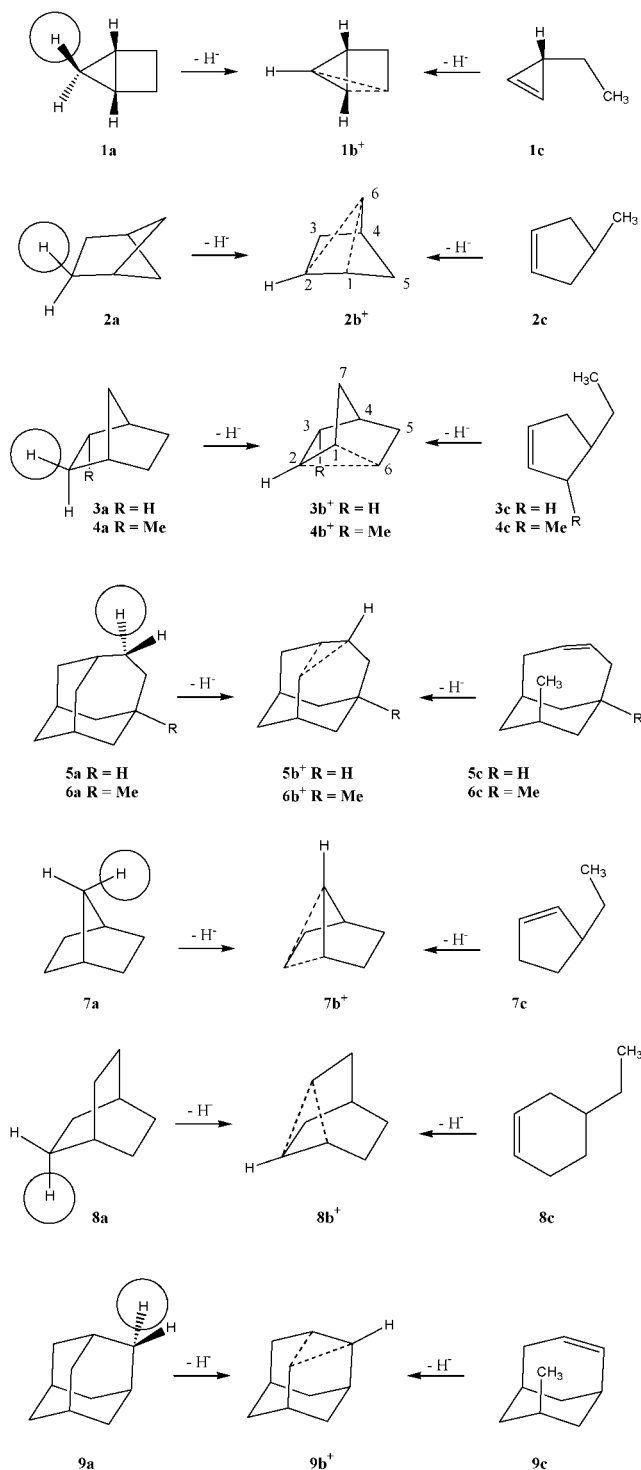
Figure 1. Compounds and ions examined

methods of choice for geometries, NMR chemical shifts and IR vibrational frequencies of carbocations.[14a,31] These calculations are generally in very good agreement with experimental data or values computed at higher levels, say QCISD. As shown below, for systems relevant to this study, NMR shifts obtained using the MP2/6–311G(d,p) level favorably compare with those obtained using DFT methods. Further, as indicated in the

Introduction, this level of computation has given us very satisfactory results in terms of computing changes of thermodynamic state functions involving hydride or chloride exchanges between carbocations.

All the *ab initio* calculations were performed with the Gaussian 98 program.[32] The structures were initially optimized at the B3LYP/6–31G* level,[33,34] frequency calculation (no imaginary frequencies) indicating that the geometries obtained are minimum structures. Additional optimizations were carried out at the MP2/6–311G** level.[35,36]

The electron density obtained at the MP2/6–311G** level was characterized using the Atoms in Molecules (AIM) methodology[37] and the AIMPAC set of programs.[38] The AIM methodology provides a unique tool to characterize atomic bonding. The electron density of a system is mathematically analyzed to find critical points (points where the gradients vanish). The presence of a $(3, -1)$ critical point known as a bond critical point (bcp) corresponds to the minimum value of the electron density in the bond path that links two nuclei. The values of the bond critical point (electron density and laplacian) are indicative of the kind of bonding, ionic or covalent. Other indices such as the ellipticity provide a quantitative description of the shape of the electron density around the bond critical points. Single bonds present ellipticities close to one, large ellipticities indicate a large π-character of the bond.

Natural Bond Orbital (NBO) analysis[39] was used to evaluate the corresponding atomic charges and to determine the nature of the molecular orbital formed with the MP2/6–311G** wavefunction. These calculations were performed with the NBO 5 version of the program.[40] The NBO method provides atomic charges, bond orders and atomic contributions to the molecular orbitals.

The values of the absolute nuclear shieldings were calculated using the GIAO method[41] at the MP2/6–311G** computational level.

RESULTS AND DISCUSSION

Geometric aspects

For the sake of conciseness we only present the optimized geometries of ions $3b^+$, $4b^+$, $6b^+$ and $9b^+$ (Fig. 2). All other geometries are given as Supporting Material.

Cations $1b^+$, $2b^+$, $3b^+$ and $5b^+$ are of C_s symmetry whereas the symmetry of $7b^+$, $8b^+$ and $9b^+$ (and also that of the derivatives $4b^+$ and $6b^+$) is C_1.
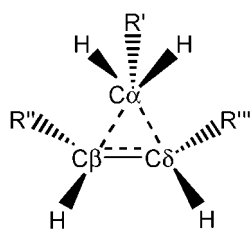
All these geometries have a common characteristic, the existence of a 'non-classical moiety' (NCM), presented in Fig. 3.

The geometries of the cation considered shows small variations in the NCM (Fig. 3 and Table 1). In this paper, the Cβ and Cδ atoms have been defined as C$\alpha\cdots$Cβ $\leq$C$\alpha\cdots$Cδ.
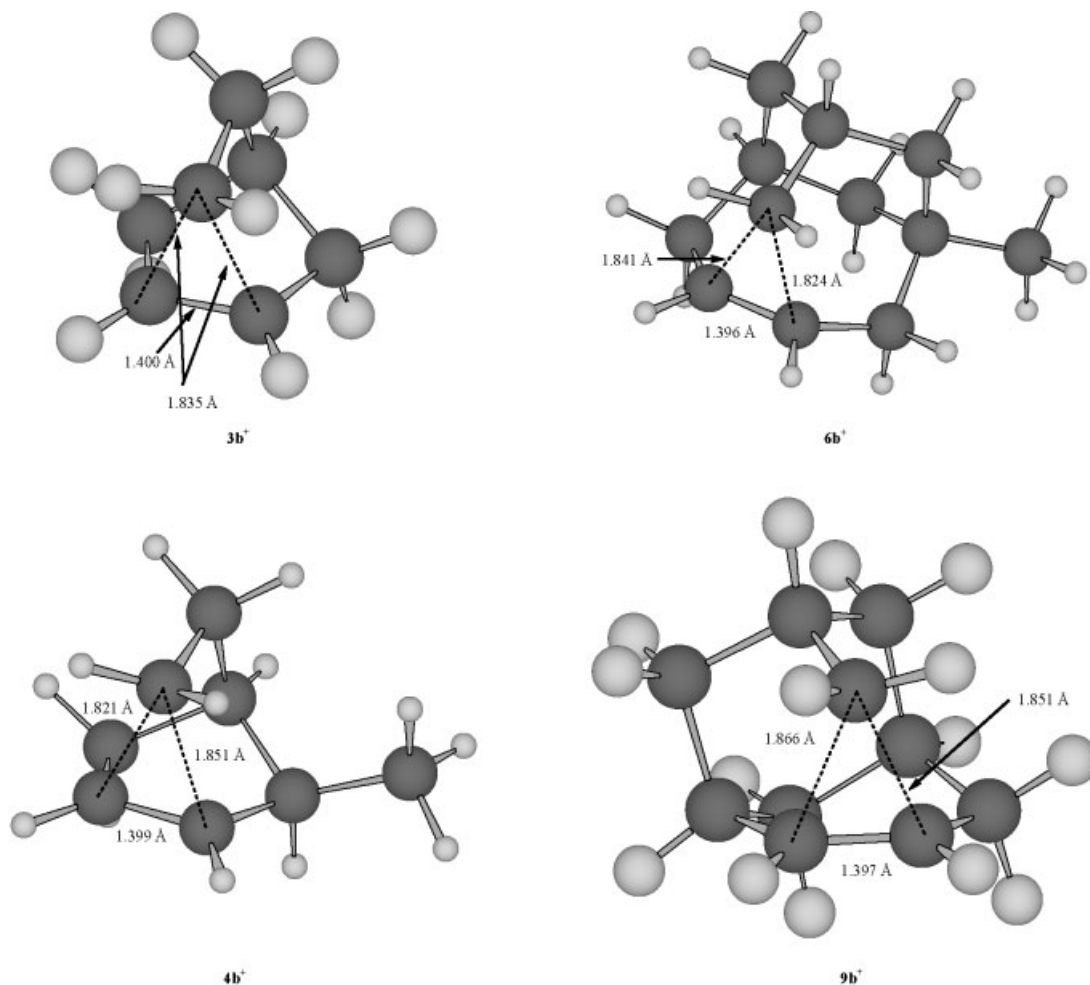
Figure 2. Optimized geometries of **3b**$^+$, **4b**$^+$, **6b**$^+$ and **9b**$^+$ at the MP2/6–311G** computational level

The average value of the C$\alpha\cdots$Cβ and C$\alpha\cdots$Cδ distances is 1.84 Å, the extreme values being those in **5b**$^+$ with the longest (1.89 Å) and the shortest (1.79 Å) interatomic distances. If the average value of each distance is considered, they are seen to range between 1.82 and 1.88 Å, an indication that a compensation effect is observed. The Cβ—Cδ bond varies between 1.39 and 1.40 Å, excluding the value in **1b**$^+$ where it is part of a strained three-membered ring. This interatomic distance is slightly larger than that obtained for the double bond of the *cis*-2-butene system (1.34 Å) calculated in this work at the MP2/6–311G** computational level.

The C_s symmetry of the carbocations of **3** and **5** is broken by methylation (**4** and **6**, respectively) even in positions located far from the NCM (Fig. 3). The resulting C$\alpha\cdots$Cβ and C$\alpha\cdots$Cδ bonds became slightly shorter and larger, respectively, than in the parent carbocations.

We finally note that cation **9b**$^+$ also displays the NCM and this fully confirms the suggestion by Esteves *et al.*[22]

Table 1. Interatomic distances (Å) in the non-classical moiety calculated at the MP2/6–311G** computational level

Cation	C$\alpha\cdots$Cβ	C$\alpha\cdots$Cδ	Cβ—Cδ
1b$^+$	1.819	1.819	1.352
2b$^+$	1.878	1.878	1.398
3b$^+$	1.835	1.835	1.400
4b$^+$	1.821	1.851	1.399
5b$^+$	1.834	1.834	1.397
6b$^+$	1.824	1.841	1.396
7b$^+$	1.793	1.887	1.393
8b$^+$	1.822	1.831	1.399
9b$^+$	1.851	1.866	1.397

Figure 3. Schematic representation of the non-classical moiety

Table 2. Relative energies (kJ mol^{-1}) of the neutral systems R$_a$ and R$_b$**CH$_3$** and energetics of reactions (2–5)[a] calculated at the MP2/6–311G** level
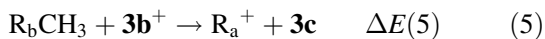
System	Relative energy of R$_a$ vs R$_b$**CH$_3$**[b]	$\Delta E(2)$	$\Delta E(3)$	$\Delta E(4)$[c]	$\Delta E(5)$
1	−84.90	1247.28	1162.38	164.71	143.20
2	31.67	1119.73	1151.40	37.16	132.22
3	−63.39	1082.57	1019.18	0.00 (0.00)	0.00
4	−68.71	1074.90	1006.19	−7.67	−12.99
5	−121.38	1076.05	954.67	−6.52 (−16.3)	−64.51
6	−122.65	1071.85	949.20	−10.72	−69.98
7	−64.81	1160.68	1095.86	78.11 (82.0)	76.68
8	−75.28	1082.15	1006.86	−0.42	−12.32
9	−118.73	1104.57	985.84	22.00 (15.5)	−33.34

[a] Defined in the text.
[b] Negative values indicate that the R$_a$ species is more stable than the R$_b$**CH$_3$** species.
[c] In parentheses, experimental values of $\Delta_r H(3)$ from data in Refs 1b and 5.

Energetic aspects

The neutral hydrocarbon precursors of the carbocations are shown in Fig. 1 (species labeled **a**). In addition, alternative potential precursor systems which include a double bond and a methyl group as responsible of the formation of the non-classical moiety have been considered (species labeled **c**).

For discussion purposes, it is useful to consider reactions (2)–(5). Reactions (2) and (3) are hydride losses from the neutral precursors **a** and **c** to yield the relevant **b**$^+$ ions. Reactions (4) and (5) provide quantitative rankings of stabilities of the various ions relative to **3b**$^+$, arbitrarily taken as a reference.

$$R_aH \rightarrow R_a{}^+ + H^- \qquad \Delta E(2) \qquad (2)$$

$$R_bCH_3 \rightarrow R_a{}^+ + H^- \qquad \Delta E(3) \qquad (3)$$

$$R_aH + 3b^+ \rightarrow R_a{}^+ + 3a \qquad \Delta E(4) \qquad (4)$$

$$R_bCH_3 + 3b^+ \rightarrow R_a{}^+ + 3c \qquad \Delta E(5) \qquad (5)$$

The relative energies of the carbocations and the corresponding neutral species and as the energetics of reactions (2)–(5) are given in Table 2. Immediate conclusions derived from this table are as follows:
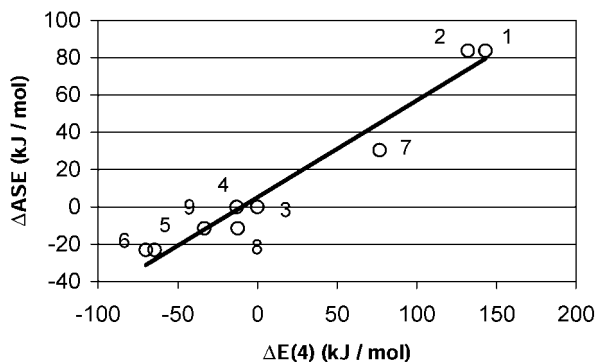
1. The results obtained show that in all the cases studied the saturated neutral precursor is more stable than the ethylenic one, with the exception of **2**. In this particular case, **2a** bears a 'bicyclobutyl-like' moiety, known to be highly strained.[42] The cyclic moiety in **2c** is a feebly strained cyclopentene (strain energy ca 10.5 kJ mol^{-1}).
2. The rankings of relatives stabilities obtained from the two families of precursors follow the same general trend.
3. On account of the isodesmic character of reaction (4), $\Delta E(4)$ values can be expected to be reasonably close to the experimental standard enthalpy changes for reaction (4), $\Delta H°(4)$. The latter data are available for

systems **3**, **5**, **7** and **9** and are reported in Table 2. The agreement is fair and suggests that our computational level is sufficient for our present purposes. In the case of **5**, the difference reaches some 10 kJ mol^{-1} *but* the difference between the experimental and computed values of $\Delta H°(4)$ is only − 5 kJ mol^{-1}.
4. The range of structural effects is large, 172.4 and 213.2 kJ mol^{-1}, respectively, depending on whether the saturated or ethylenic precursors are chosen (see Table 2).
5. Reaction (5) helps shed light on the origin of the wide span of structural effects on the stability of these species. Consider, for example, the formation of **3b**$^+$ starting from **3c**. Formally, this can be achieved by hydride abstraction from the methyl group in **3c** followed by the approach of the resulting cation to the double bond to yield **3b**$^+$. The latter ion can be described by the two mesomeric structures **3b**$^+$$_I$ and **3b**$^+$$_{II}$ shown in Fig. 4. They both present a five-membered ring.

Similar reasoning applies to the formation of **7b**$^+$, as

3b$^+$ **3b**$^+$$_I$ **3b**$^+$$_{II}$

7b$^+$ **7b**$^+$$_I$ **7b**$^+$$_{II}$
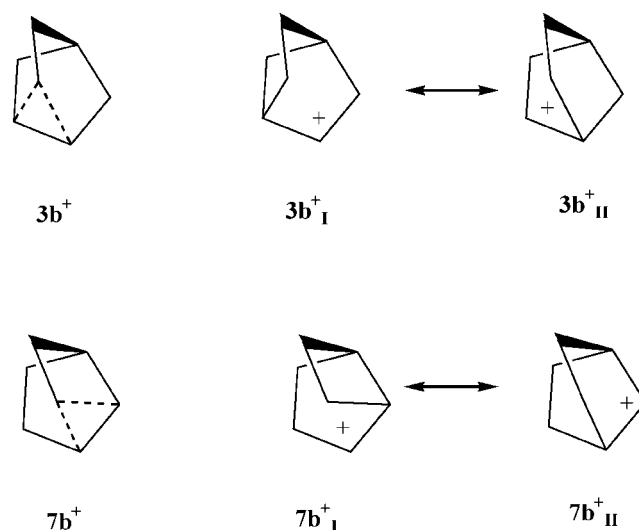
Figure 4. Mesomeric structures of **3b**$^+$ and **7b**$^+$

Figure 5. ΔASE vs $\Delta E(5)$. The fitted straight line corresponds to the equation ΔASE $= 5.13 + 0.52\Delta E(5)$, $R^2 = 0.96$

Table 4. Electron density properties at the bond critical point of the $C\alpha\cdots C\beta$ bond

System	ρ (a.u.)	$^2\rho$ (a.u.)	Ellipticity	Bond path length minus geometrical bond length. (Å)
1b$^+$	0.129	0.021	6.50	1.151
2b$^+$	0.116	0.033	4.32	1.205
3b$^+$	0.127	0.013	6.72	1.220
4b$^+$	0.143	0.002	3.65	0.251
5b$^+$	0.126	0.011	6.37	1.174
6b$^+$	0.127	0.007	5.27	0.364
7b$^+$	0.130	-0.025	1.80	0.186
8b$^+$	0.128	0.007	5.79	0.440
9b$^+$	0.130	-0.052	2.97	0.475

described by structures $\mathbf{7b}^+_I$ and $\mathbf{7b}^+_{II}$ (see Fig. 4). Relative to **7c** they present one four- and one six-membered ring, respectively. Obviously, the actual geometries of the ions are intermediate between the two extremes and are affected by other factors, as discussed above. Here we assume, for simplicity, that the difference in stability between two of the ions examined here is given to a large extent by the difference in their strain energies relative to their neutral precursors. We also assume that for each ion, the main contribution to this strain energy is given by the average of the strain energies (ASE) pertaining to the formation of the structures I and II starting from the corresponding ethylenic precursors. Here we use the strain energies reported by Burkert and Allinger[43] for cyclobutane, cyclopentane and cyclohexane, 117.76, 33.97 and 10.92 kJ mol^{-1}, respectively. In the case of $\mathbf{3b}^+$ and $\mathbf{7b}^+$ the ASE values thus estimated are 33.97 and 64.34 kJ mol^{-1}, respectively. Figure 5 is a plot of $\Delta E(5)$ against ΔASE, the difference between the ASE for any ion and ASE for $\mathbf{3b}^+$.

The correlation between $\Delta E(5)$ and ΔASE is surprisingly good, in spite of the crude model that we used (highly sophisticated molecular mechanics methods have recently been used for carbocations[44] although, to our knowledge, they have not yet been systematically applied to non-classical ions). Here we just intended to indicate

that these effects are important in this family of ions. The slope of the correlation, ca 0.5, seems to indicate that a significant part of the differential structural effects does indeed originate in the strain of the carbocations. The study of the influence of strain on the reactivity of carbocations in solution has a long history[45] and has been quantified and determined experimentally in a number of cases.[1] Here we show that it is also a fundamental factor determining the relative stabilities of non-classical ions.

6. The introduction of a methyl group near the NCM leads to a small increase in the stability of the carbocation. This effect, larger the closer the substituent, is a well known feature of gas-phase stabilities and is generally attributed to a 'polarizability effect.'[46]

Electronic aspects

The charges summed over the heavy atoms, the bond order and the atomic contribution to the two-electron, three-center orbital obtained with the NBO methodology for the three groups involved in the NCM are given in Table 3.

Table 3. Charges (e), bond order and % atomic contribution to the two electron, three center orbital calculated with the NBO methodology at the MP2/6–311G** level

	Charge		Bond order		% atomic contribution to the two-electron, three center orbital	
System	$C\alpha H_2$	$C\beta H/C\delta H$	$C\alpha\cdots C\beta/C\alpha\cdots C\delta$	$C\beta$—$C\delta$	$C\alpha$	$C\beta/C\delta$
1b$^+$	0.296	0.260	0.48	1.25	37.06	31.47
2b$^+$	0.276	0.262	0.44	1.26	36.19	31.90
3b$^+$	0.253	0.241	0.47	1.20	38.56	30.72
4b$^+$	0.249	0.225/0.258	0.49/0.45	1.20	38.68	31.94/29.38
5b$^+$	0.243	0.233	0.48	1.20	39.03	30.49
6b$^+$	0.259	0.241/0.249	0.49/0.47	1.19	39.04	31.06/29.91
7b$^+$	0.259	0.241/0.249	0.49/0.44	1.23	37.21	32.16/30.62
8b$^+$	0.254	0.232/0.237	0.48/0.47	1.20	38.50	30.99/30.51
9b$^+$	0.246	0.233/0.247	0.46/0.45	1.22	37.80	31.50/30.70
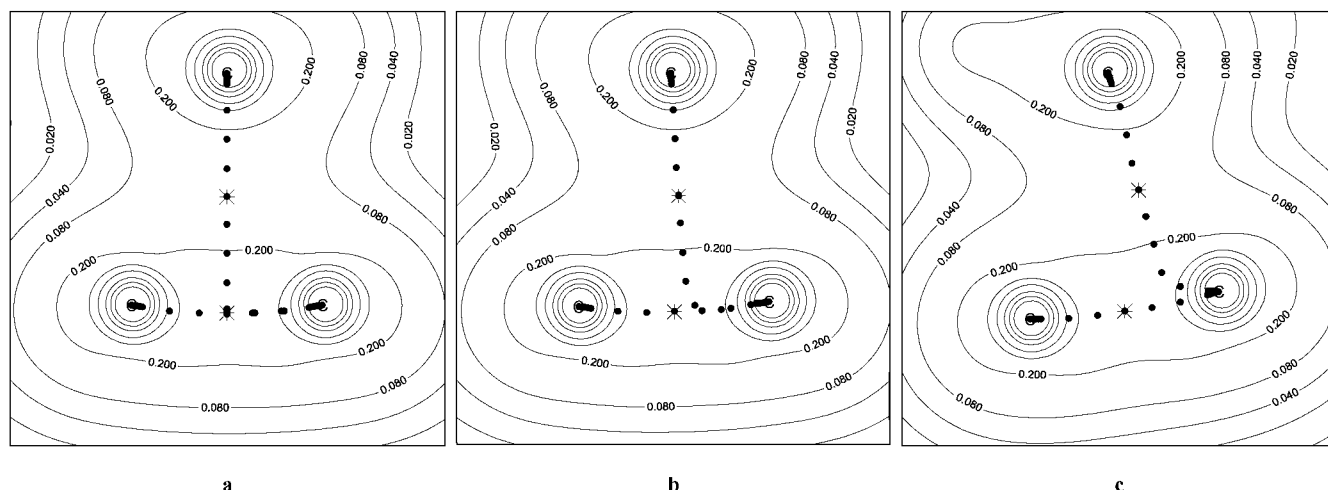
Figure 6. Electron density maps of (a) **5b**[+], (b) **6b**[+] and (c) **7b**[+] (a.u.). The stars indicate the position of the bond critical points and the dots the bond path

The charge distribution obtained shows how the NCM efficiently distributes the positive charge between the three groups with an almost identical value for each one, in all the cases the positive value of CαH$_2$ being slightly larger than the other two. In addition, a small amount of charge, that ranges between 0.18e and 0.29e in the carbocations studied, is spread over the rest of the molecule.

The atomic contribution to the two-electron, three-center orbitals obtained follows the same trend as the atomic charges. The values are similar for the three carbon atoms that define the NCM, in all the cases the Cα contribution being the largest. In the non-symmetrical cases, the Cβ contribution is always larger than the Cδ contribution.

The bond order shows that the C$\alpha\cdots$Cβ and C$\alpha\cdots$Cδ contacts range between 0.44 and 0.49, i.e. half that of a standard single C—C bond. For Cβ—Cδ, the values are between 1.20 and 1.26, which is an intermediate value between a standard single C—C bond and a double bond (for comparative purposes the bond orders of *cis*-2-butene and ethane at the same computational level are 1.78 and 0.98, respectively)

In all the cases studied, the analysis of the electron density shows only one bond critical point, located between the Cα and the Cβ—Cδ groups (Table 4). The values of the electron density and its laplacian indicate that the interactions discussed above are at the borderline between shared-shell and closed-shell interactions.[47] The large value of the ellipticity in the bcps indicates that the electron density surface in their vicinity is rather flat. Even the smallest value obtained (1.80 for **7b**[+]) is much larger than those obtained for standard CC bonds, in the range 0–0.5.[48]

In the case of the symmetrical cations (**1–3** and **5**), a T-shaped bond path [Fig. 6(a)] is obtained similar to that previously described for the 2-norbornyl cation.[14a,c] The bond path linking the Cα atom and the Cβ/Cδ atoms goes through the center of their bond and bifurcates at that point. Since the electron density map corresponds to a

Table 5. Calculated ^{13}C chemical shielding (ppm) relative to TMS[a] at the GIAO//MP2/6–311G** computational level

System	Cα	Cβ/Cδ	System	CH$_3$	Cβ/Cδ
1b[+]	38.97	125.12	**1c**	14.22	112.53
2b[+]	75.23	157.95	**2c**	22.28	132.66
3b[+]	24.33	126.69	**3c**	10.67	131.95
4b[+]	22.92	121.64/137.39	**4c**	14.43	131.27/138.27
7b[+]	36.56	132.39/127.96	**7c**	10.06	136.34/133.41
8b[+]	31.43	132.82/123.29	**8c**	15.68	129.82/130.01
9b[+]	48.58	132.64/145.05	**9c**	26.65	131.16/137.47

[a] The calculated absolute value of the ^{13}C of TMS is 198.98.

Table 6. Experimental and calculated (at the GIAO//MP2/6–311G** level) ^{13}C chemical shieldings (ppm) relative to TMS for ions **2b**[+] and **3b**[+a]

Ion	Chemical shifts			
	Exp.[b]	Absolute value[c]	Rel. TMS[c]	Lit. values[d]
2b[+]				
C1,2	157.8	41.03	157.95	158.5
C3,5,6(av)	49.1	146.72	52.26	45.7
C4	43.4	149.82	49.16	37.5
3b[+]				
C1,2	124.5	72.29	126.69	137.1
C3,7	36.3	157.87	41.11	41.38
C4	37.7	156.47	42.51	47.28
C5	20.4	174.55	24.43	23.04
C6	21.2	176.64	24.33	37.68

[a] Carbon atoms numbered as in in Fig. 1.
[b] Experimental data for **2b**[+] and **3b**[+] from Refs (M) and (W), respectively.
[c] Computed, this work.
[d] Computed values for **2b**[+] (IGLO, DZ//MP2FULL/6–31G*) and **3b**[+] [CSGT, B3LYP/6–311+G(d,p)] are from Refs 14b and 12c, respectively.

catastrophic situation, any small change that distorts the symmetry induces the formation of a unique bond between the Cα atom and Cβ or Cδ atom [Fig. 6(b)].[14b,d] This is the case for the methyl derivatives of **3b**$^+$ and **5b**$^+$, which correspond to the structures **4b**$^+$ and **6b**$^+$, respectively. Hence the effective electron density map of these systems shows a tetracoordinated carbocation. Similar catastrophic electron density maps have been described for hydrogen-bonded complexes where π-systems act as acceptors.[49]

Even though a single bond path is obtained between the Cα and the Cβ—Cδ groups in the non-symmetrical cations (**4b**$^+$, **5b**$^+$–**9b**$^+$) linking Cα and Cβ, a clear influence of the Cδ atom is observed due to the curvature of the bond path (Fig. 6). Thus, significant values are obtained in all cases for the difference between the electronic bond path and the interatomic distance (Table 4). A similar effect but on a smaller scale is observed in bent bonds of strained three-membered rings.

NMR aspects

The chemical shieldings of the NCM carbon atoms calculated at the MP2/6–311G** level with the GIAO methods are given in Table 5. For comparative purposes, the same carbon atoms in the **c** species are included. We present in Table 6 a detailed comparison of our computed chemical shifts with the available experimental and computational values from the literature. As can be seen, our results agree with the experimental values within an average unsigned difference of 3.2 ppm, the correlation between experimental and calculated values being excellent ($r^2 > 0.999$).

The results obtained for the carbocations and **c** species are very similar and in all cases the values for the former are larger (up to 50 ppm) than those for the latter neutral species. These differences can be explained on the basis of a similar distribution of the positive charge over the three atoms of the NCM as discussed previously. For the sake of comparison, the ^{13}C chemical shielding of the simplest neutral–cation pair with a positive carbon atom (methane and methyl cation) was calculated at the same computational level and shows a difference of almost 400 ppm (-3.22 and 385.59 ppm, respectively)

Thus, the Cα atom of the carbocations and the CH$_3$ of the **c** series show chemical shieldings characteristic of saturated hydrocarbons and the Cβ and Cδ atoms in both systems are in the range of double bonds.

CONCLUSIONS

We have examined nine bi- and tricyclic carbocations having 5–11 carbon atoms in their cyclic frameworks. All of them have in common a fundamental geometric feature, the non-classical moiety portrayed in Fig. 2. The

three relevant bond lengths of the NCM were found to vary between rather narrow limits. This indicates that the NCM provides an efficient means to stabilize these ions even though the sizes of the various systems are very different. Our computational results show indeed that it allows a very efficient charge dispersal and that this is smoothly achieved following the hydride abstraction from hydrocarbon precursors. As regards the structure of the NCM, we find that the atomic contribution to the two-electron, three-center orbitals is of the same order of magnitude for all three carbon atoms. The electron density maps show two bond paths between the three carbon atoms involved in the NCM moiety with one of them very curved owing to the influence of the additional atom. Their computed chemical shieldings reveals that Cα and the couple Cβ/Cδ are rather similar to saturated and ethylenic hydrocarbons, respectively.

REFERENCES

1. (a) Abboud JLM, Herreros M, Notario R, Lomas JS, Mareda J, Müller P, Rossier JC. *J. Org. Chem.* 1999; **64**: 6401; (b) Abboud JLM, Castaño O, Della EM, Herreros M, Müller P, Notario R, Rossier JC. *J. Am. Chem. Soc.* 1997; **119**: 2262.
2. (a) Abboud JLM, Castaño O, Elguero J, Herreros M, Jagerovic N, Notario R, Sak K. *Int. J. Mass Spectrom. Ion Processes* 1998; **175**: 35; (b) Takeuchi K, Takasuka M, Shiba E, Kinoshita T, Okazaki T, Abboud JLM, Notario R, Castaño O. *J. Am. Chem. Soc.* 2000; **122**: 7351.
3. Abboud JLM, Castaño O, Herreros M, Leito I, Notario R, Sak K. *J. Org. Chem.* 1998; **63**: 8995.
4. Abboud JLM, Alkorta I, Dávalos JZ, Müller P, Quintanilla E. *Adv. Phys. Org. Chem.* 2002; **37**: 57.
5. Abboud JLM, Castaño O, Dávalos JZ, Jiménez P, Gomperts R, Müller P, Roux MV. *J. Org. Chem.* 2002; **67**: 1057.
6. Abboud JLM, Alkorta I, Dávalos JZ, Müller P, Quintanilla E, Rossier JC. submitted.
7. Arnett EM, Petro C, Schleyer PvR. *J. Am. Chem. Soc.* 1979; **101**: 522.
8. Schreiner PR, Schleyer PvR, Schaeffer HF III. *J. Org. Chem.* 1997; **62**: 4216.
9. Arnett EM, Abboud JLM. *J. Am. Chem. Soc.* 1975; **97**: 3865.
10. (a) Baer T, Song Y, Ng C, Liu J, Chen W. *J. Phys. Chem. A* 2000; **104**: 1959; (b) Abboud JLM, Castaño O, Dávalos JZ, Gomperts R. *Chem. Phys. Lett.* 2001; **337**: 327.
11. Brown HC (with comments by Schleyer PvR). *The Nonclassical Ion Problem*. Plenum Press: New York, 1977; 50.
12. Meerwein H, van Emster K. *Chem. Ber.* 1922; **55**: 2500.
13. Brunelle P, Sorensen, TS, Taeschler C. *J. Org. Chem.* 2001; **66**: 7294.
14. (a) Werstiuk NH, Muchall HM. *THEOCHEM* 1999; **463**: 225; (b) Werstiuk NH, Muchall HM *J. Phys. Chem. A* 1999; **103**: 6599; (c) Werstiuk NH, Muchall HM. *J. Phys. Chem. A* 2000; **104**: 2054; (d) Werstiuk NH, Muchall HM, Stephane N. *J. Phys. Chem. A* 2000; **104**: 11601; (e) Werstiuk NH, Wang YG. *J. Phys. Chem. A* 2001; **105**: 11515.
15. Olah GA, Liang G, Jindal SP. *J. Am. Chem. Soc.* 1976; **98**: 2508.
16. (a) Schleyer PvR, Ladig K, Schindler M. *J. Am. Chem. Soc.* 1988;

110: 2508; (b) Schleyer PvR, Laidig K, Wiberg KB, Saunders M, Schindler M. *J. Am. Chem. Soc.* 1988; **110**: 300.

17. Winstein S, Carter P. *J. Am. Chem. Soc.* 1961; **83**: 4485.
18. Mesic M, Sunko DE, Vancik H. *J. Chem. Soc., Perkin Trans. 2* 1994; 1135.
19. (a) Sieber, S, Schleyer PvR, Vancik H, Mesic M, Sunko DE. *Angew. Chem., Int. Ed. Engl.* 1993; **32**: 1604; (b) 1993; **32**: 1606.
20. Walborsky HM, Baum ME, Youssef A. *J. Am. Chem. Soc.* 1961; **83**: 988.
21. Goering HL, Sloan MF. *J. Am. Chem. Soc.* 1961; **83**: 1397.
22. Esteves PM, Alberto GGP, Ramirez-Solis A, Mota CJA. *J. Phys. Chem. A* 2001; **105**: 4308.
23. (a) Dutler R, Rauk A, Sorensen TS, Whitworth SM. *J. Am. Chem. Soc.* 1989; **111**: 9024; (b) Sorensen TS. In *Stable Carbocation Chemistry*, Surya Prakash GK, Schleyer PvR (eds). Wiley: New York, 1997; 75–136.
24. (a) Winstein S, Trifan DS. *J. Am. Chem. Soc.* 1949; **71**: 2953; (b) Schleyer PvR. *J. Am. Chem. Soc.* 1989; **111**: 9024; (c) Grob C. *Acc. Chem. Res.* 1983; **16**: 426; (d) Olah GA, Surya Prakash GK, Saunders M. *Acc. Chem. Res.* 1983; **16**: 440; (d) Brown HC. *Acc. Chem. Res.* 1983; **16**: 432.
25. Olah GA, Surya Prakash GK, Arvanaghi M, Anet FAL. *J. Am. Chem. Soc.* 1982; **104**: 7105.
26. Yannoni CS, Macho V, Myhre PC. *J. Am. Chem. Soc.* 1982; **104**: 7380.
27. Koch W, Liu B, DeFrees DJ, Sunko DE, Vancik H. *Angew. Chem., Int. Ed. Engl.* 1990; **29**: 183.
28. Johnson SA, Clark DT. *J. Am. Chem. Soc.* 1988; **110**: 4112.
29. Schreiner PR, Severance DL, Jorgense WL, Schleyer PvR, Schaefer HF III. *J. Am. Chem. Soc.* 1995; **117**: 2663.
30. Maerker C. PhD Thesis, University of Erlangen, 1997.
31. Schelyer PvR, Maerker C. *Pure Appl. Chem.* 1995; **67**: 755.
32. Frisch MJ, Trucks GW, Schlegel HB, Scuseria GE, Robb MA, Cheeseman JR, Zakrzewski VG, Montgomery JA, Stratmann RE, Burant JC, Dapprich S, Millam JM, Daniels AD, Kudin KN, Strain MC, Farkas O, Tomasi J, Barone V, Cossi M, Cammi R, Mennucci B, Pomelli C, Adamo C, Clifford S, Ochterski J, Petersson GA, Ayala PY, Cui Q, Morokuma K, Malick DK, Rabuck AD, Raghavachari K, Foresman JB, Cioslowski J, Ortiz JV, Stefanov BB, Liu G, Liashenko A, Piskorz P, Komaromi I, Gomperts R, Martin RL, Fox DJ, Keith T, Al-Laham MA, Peng CY, Nanayakkara A, González C, Challacombe M, Gill PMW, Johnson BG, Chen W, Wong MW, Andrés JL, Head-Gordon M, Replogle ES, Pople JA. Gaussian 98. Gaussian: Pittsburgh, PA, 1998.
33. (a) Becke AD *J. Chem. Phys.* 1993; **98**: 5648; (b) Lee C, Yang W, Parr RG. *Phys. Rev. B* 1988; **3**: 785.
34. Hariharan PA, Pople JA. *Theor. Chim. Acta* 1973; **28**: 213.
35. Møller C, Plesset MS. *Phys. Rev.* 1934; **46**: 618.
36. Frisch MJ, Pople JA, Krishnam R, Binkley JS. *J. Chem. Phys.* 1984; **80**: 3265.
37. Bader RFW. *Atoms in Molecules: A Quantum Theory*. Clarendon Press: Oxford, 1990.
38. Bieger-Konig FW, Bader RFW, Tang THJ. *J. Comput. Chem.* 1982; **3**: 317.
39. Reed AE, Curtiss LA, Weinhold F. *Chem. Rev.* 1988; **88**: 899.
40. Glendening ED, Badenhoop K, Reed AE, Carpenter JE, Bohmann JA, Morales CM, Weinhold F. NBO 5.0. Theoretical Chemistry Institute, University of Wisconsin, Madison, WI, 2001.
41. Ditchfield R. *Mol. Phys.* 1974; **27**: 789; London F. *J. Phys. Radium* 1937; **8**: 397.
42. Politzer P, Kirschenheuter GP, Alster J. *J. Am. Chem. Soc.* 1987; **109**: 1020.
43. Burkert U, Allinger NI. *Molecular Mechanics*. ACS Monograph 177. American Chemical Society: Washington, DC, 1982; 188.
44. Reindl B, Clark T, Schleyer PvR. *J. Phys. Chem. A* 1998; **102**: 8953.
45. (a) Foote CS. *J. Am. Chem. Soc.* 1964; **86**: 1853; (b) Schleyer PvR. *J. Am. Chem. Soc.* 1964; **86**: 1854, 1856; (c) Bingham CR, Schleyer PvR. *J. Am. Chem. Soc.* 1971; **93**: 3189; (d) Parker W, Trauter RL, Watt CIF, Chang LWK, Schleyer PvR. *J. Am. Chem. Soc.* 1974; **96**: 7121; (e) Müller P, Blanc J, Mareda J. *Chimia* 1984; **38**: 389.
46. Taft RW, Topsom RD. *Prog. Phys. Org. Chem.* 1987; **16**: 1.
47. Espinosa E, Alkorta I, Elguero J, Molins E. *J. Chem. Phys.* 2002; **117**: 5529.
48. Popelier P. *Atoms in Molecules. An Introduction*. Prentice Hall: Singapore, 2000; 148.
49. Rozas I, Alkorta I, Elguero J. *J. Phys. Chem.* 1997; **101**: 9457.